SEEBECK COEFFICIENT MEASUREMENT BY KELVIN-PROBE FORCE MICROSCOPY

Hiroya Ikeda, Faiz Salleh, Kiyosumi Asai

Abstract:

In order to measure the Seebeck coefficient of nanometer-scale thermoelectric materials, we propose a new technique in which the thermoelectric-motive force (TEMF) is evaluated by Kelvin-probe force microscopy (KFM). In this study, we measured the Seebeck coefficient of an n-type Si wafer. The surface-potential difference between the high- and low-temperature regions on the Si wafer increases with increasing temperature difference. This indicates that the TEMF can be measured by KFM. The Seebeck coefficient evaluated from the surface-potential difference is 0.71±0.08 mV/K, which is close to that obtained by the conventional method.

Keywords: *Seebeck coefficient, Kelvin-probe force microscopy, nanostructure.*

1. Introduction

The introduction of nanometer-scale structures into thermoelectric materials has been expected to lead to breakthroughs for enhancing the thermoelectric figure-of-merit [1]-[4]. A number of researchers are engaged in characterizing nanometer-scale thermoelectric materials [5]-[8]. However, it is very difficult to measure the thermoelectric characteristics of these materials because of the very small dimensions. External disturbances such as lead-wire contact essential to the conventional thermo-electric-motive force (TEMF) measurement affect accurate evaluation. Recently, probe microscopy techniques have attracted significant attention for the thermoelectric characterization of nanometer-scale materials [9], [10]. In these techniques, a probe is contacted with the sample surface and thermoelectric characterization is performed on the basis of the vertical temperature difference (i.e. normal to the sample surface). Therefore, contact of the metallic probe with the sample surface cannot be avoided, and specially-customized equipment is needed.

We propose a new technique using Kelvin-probe force microscopy (KFM) for Seebeck coefficient measurement. Using this technique, it is possible to obtain the work-function difference between the cantilever and the sample, that is, the Fermi energy of the sample relative to that of the cantilever metal. Consequently, TEMF can be obtained from the Fermi energies at the high- and low-temperature regions. This allows for evaluation of the Seebeck coefficient of the sample. One of the crucial advantages to be emphasized of this technique is that the cantilever never touches the sample surface during the measurement. Therefore, the TEMF measurement is not perturbed by external factors such as the metallic probe and the lead wire. Another advantage is that we can use commercial KFM equipment by adjustments of the sample holder. In the present report, we demonstrate the use of KFM for the measurement of the Seebeck coefficient of a bulk Si wafer and show that KFM can be a powerful tool for characterizing the Seebeck coefficient of nanometer-scale materials.

2. Experimental

Figure 1 shows a schematic of the experimental setup. Two Cu plates were placed side by side with a gap of 4 mm. A resistive heater was attached to one of the Cu plates. An n-type Si wafer, with an impurity concentration of $1x10^{18}$ cm-3 cut to a size of 5 x10 mm^2, was bridged over these Cu plates and attached using conductive Ag-paste. By heating one side of the sample, a temperature difference is produced in a plane parallel to the sample surface. Two K-type thermocouples were directly attached to the sample surface. Time evolution of the surface potential was measured by KFM equipment (Seiko Instruments Inc. SPI 3800N) and monitored by a digital multimeter (HIOKI HiLOGGER 8430), simultaneous with temperature measurement at the high- and low-temperature regions on the sample surface. The KFM cantilever was made of Si coated with Au. Surface-potential measurements were carried out in a vacuum chamber (Seiko Instruments Inc. SPA-300HV) with a pressure of $2.5x10^{-5}$ Pa.

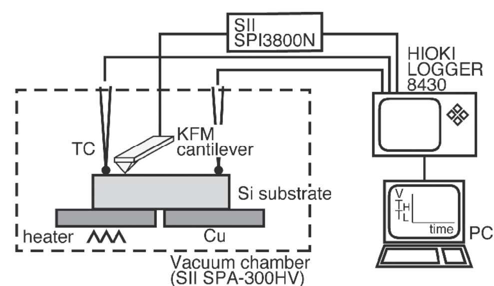

Fig. 1. Schematic diagram of the apparatus for Seebeck coefficient measurements by KFM.

3. Results and Discussions

The time evolution of the surface potential in the high-temperature region and of the temperature at the high- and low-temperature regions on the n-type Si wafer are shown in Figs. 2(a) and 2(b), respectively. Unfortunately, the KFM measurement could not sufficiently follow the time evolution of the surface potential due to overflow in the z-gain during the elevation of the temperature. In this study, therefore, we heated the sample step-by-step and measured the surface potential only at

each stable-temperature region. During the elevation of the temperature, the cantilever was kept away from the sample. By this procedure, a pulse-like signal was obtained for the surface potential and staircase-shaped curves were obtained for the temperature time-evolution, as shown in Fig. 2. Similarly, the surface potential at the low-temperature region was also obtained. It is seen in Fig. 2(a) that the surface potential is relatively stable during the KFM detection. However, the surface potential has a finite value even during the measurement break. This is likely due to parasitic potential originating from the equipment, which needs to be subtracted from the surface-potential signal.

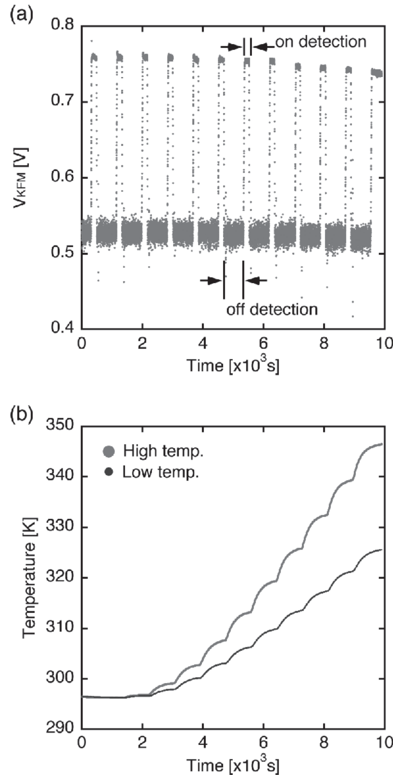

Fig. 2. Time evolution of (a) surface potential at the hith-temperature region and (b) tempera-tures at the high- and low-temperature regions on an n-type Si wafer.

Moreover, the influence of the Schottky contact at the n-type Si/Ag paste interface must also be taken into account. Figures 3(a) and 3(b) show schematic energy-band diagrams of our KFM measurement setup. Before the application of a voltage to remove the Coulomb force between the cantilever and the sample surface (V_{KFM}), our setup has the band diagram shown in Fig. 3(a) wherein all the Fermi energies of the Cu plate, the Ag paste, the n-Si and the Au coating the Si cantilever are identical. Hence, the Si band bends at the surface and the bottom, and the vacuum level slopes between the cantilever and the sample, representing the existence of the Coulomb force. After applying V_{KFM}, the vacuum level becomes flat (no Coulomb force), and there is an energy difference -eV_{KFM} between the Fermi energies of the cantilever and the Ag paste. The potential difference V_{KFM} consists of voltage drops at vacuum (ϕSi) and the Si bottom (ϕ_{add}). Since a Fermi energy difference between the cantilever and the sample -eϕSi is necessary for evaluation of the TEMF, the additional potential ϕ_{add} must be removed from the detected surface potential V_{KFM}.

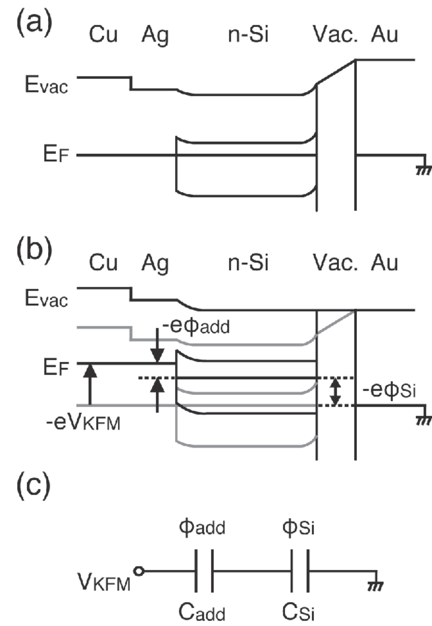

Fig. 3. Energy bands of the KFM measurement setup (a) before and (b) after application of a voltage to remove the Coulomb force between the cantilever and the sample surface V_{KFM}, and (c) simple equivalent circuit of the band diagram with V_{KFM}.

For this purpose, an equivalent circuit, shown in Fig. 3(c), is assumed for the band diagram of Fig. 3(b), where two capacitors are connected in series. In this circuit, two equations,

$$V_{KFM} = \phi_{Si} + \phi_{add} \tag{1}$$

$$C_{Si}\phi_{Si} = C_{add}\phi_{add} \tag{2}$$

are valid, where C_{Si} and C_{add} are the capacitance of vacuum and additional capacitors, respectively. These are expressed as [11]

$$C_{Si} = \frac{\varepsilon_0}{d} \tag{3}$$

$$C_{add} = \sqrt{\frac{e\varepsilon_{Si}N_D}{d(V_{bi}-\phi_{add})}}, \tag{4}$$

where d is the gap distance between the cantilever and the sample, and ND the impurity concentration in Si, ε_0 and εSi are the dielectric constant in vacuum and Si, and V_{bi} is the built-in potential at the n-type Si/Ag interface, which is expressed by

$$V_{bi} = \phi_{Ag} - \chi_{Si} - (E_C - E_F)/e \quad , \tag{5}$$

where $e\chi_{Si}$ and $e\phi_{Ag}$ are the electron affinity of Si and the work function of Ag, respectively. The surface potential ϕ_{Si} is obtained by the equation

$$\phi_{Si} = \chi_{Si} + (E_C - E_F)/e - \phi_{Au} \quad , \tag{6}$$

where $e\phi_{Au}$ is the work function of Au. The theoretical ϕ_{Si} for ΔT=0K (T=297K) is calculated using Eq. (6) to be -1.016V for N_D=1x10^{18} cm^{-3} since the system is in thermal equilibrium under this condition. Then, assuming that the vacuum gap d=9 nm, ϕ_{add} and V_{KFM} are estimated to be -0.219 and -1.235V, respectively. Here, the potential difference between the measured and calculated KFM values for ΔT=0K is likely to be due to a background potential f_{bg} originating from the measurement equipment. Therefore, the corrected KFM value can be defined as $\tilde{V}_{KFM}=V_{KFM}-f_{bg}$ unless the background potential ϕ_{bg} strongly depends on the temperature.

From Eqs. (1)-(6), the true surface potential of Si is represented as:

$$\phi_{Si} = \frac{\tilde{V}_{KFM}}{1 + C_{Si}\sqrt{\frac{2(\phi_{Ag}-\phi_{Au}-\tilde{V}_{KFM})}{e\varepsilon_{Si}N_D}}}, \quad (7)$$

which is shown in Fig. 4 for the high- and low-temperature regions (ϕ^{H}_{KSi} and ϕ^{L}_{KSi}) as a function of temperature difference. The surface-potential difference between these temperature regions is found to increase with increasing temperature difference, indicating that the TEMF can indeed be measured. Since the values of the surface potentials appear to lie on straight lines, the Seebeck coefficient is constant in this temperature range. From the gradients of these straight lines, the Seebeck coefficient was estimated to be $S=\Delta V/\Delta T=(\phi^{H}_{KSi} - \phi^{L}_{KSi})/\Delta T$ =0.71±0.08 mV/K, which is close to the value measured by a conventional method of S=0.89 mV/K [12]. This result indicates that the KFM technique indeed has the ability to evaluate the Seebeck coefficient.

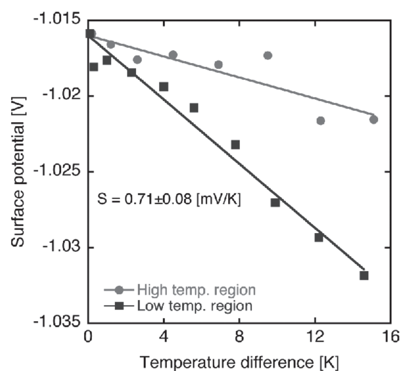

Fig. 4. Surface potentials at the high- and low-temperature regions on the n-type Si wafer as a function of temperature difference.

4. Conclusions

We have developed a new technique using KFM for measuring the Seebeck coefficient of nanometer-scale thermoelectric materials. In our present experiment, the Seebeck coefficient of an n-type Si wafer was estimated to be S=0.71±0.08 mV/K, which is close to that obtained by a conventional method. This indicates that the Seebeck coefficient can indeed be measured by KFM with no contact between the probe and the sample, leading to realization of accurate Seebeck-coefficient measurement for nanometer-scale materials.

However, some problems also come significant. The severest point is that the Seebeck coefficient evaluation in this study stands on a lot of assumptions. This makes the validity of the resultant value doubtful, especially in nanometer-scale measurements. We have to measure the Seebeck coefficient for samples with Ohmic contact in future.

ACKNOWLEDGMENTS

This work was financially supported by a Grant-in-Aid for Scientific Research (19560701 and 21360336) from the Japan Society for the Promotion of Science.

AUTHORS

Hiroya Ikeda*, Faiz Salleh, Kiyosumi Asai - Research Institute of Electronics, Shizuoka University, Johoku 3-5-1, Naka-ku, Hamamatsu 432-8011, Japan.
E-mail: ikeda@rie.shizuoka.ac.jp.
* Corresponding author

References

[1] Hicks L.D., Dresselhaus M.S., "Effect of quantum-well structures on the thermo-electric figure of merit", *Phys. Rev. B*, vol. 47, no. 19, 1993, pp. 12727-12731.
[2] Hicks L.D., Dresselhaus M.S., "Thermoelectric figure of merit of a one-dimensional conductor", *Phys. Rev. B*, vol. 47, no. 24, 1993, pp. 16631-16634.
[3] Balandin A.A., Lazarenkova O.L., "Mechanism for thermoelectric figure-of-merit enhancement in regimented quantum dot superlattices", *Appl. Phys. Lett.*, vol. 82, no. 3, 2003, pp. 415-417.
[4] Simkin M.V., Mahan G.D., "Minimum thermal conductivity of superlattices", *Phys. Rev. Lett.*, vol. 84, no. 5, 2000, pp. 927-930.
[5] Harman T.C., Taylor P.J., Walsh M.P., LaForge B.E., "Quantum dot superlattice ther-moelectric materials and devices", *Science*, vol. 297, 2002, pp. 2229-2232.
[6] Li D., Wu Y., Kim P., Shi L., Yang P., Majumdar A., "Thermal conductivity of indi-vidual silicon nanowires", *Appl. Phys. Lett.*, vol. 83, no. 14, 2003, pp. 2934-2936.
[7] Hochbaum A.I., Chen R., Delgado R.D., Liang W., Garnett E.C., Najarian M., Majumdar A., Yang P., "Enhanced thermoelectric performance of rough silicon nanowires", *Nature*, vol. 451, 2008, pp. 163-167.
[8] Boukai A.I., Bunimovich Y., Kheli J.T., Yu J.K., Goddard W.A. III, Heath J.R., "Silicon nanowires as efficient thermoelectric materials", *Nature*, vol. 451, 2008, pp. 168-171.
[9] Williams C.C., Wickramasinghe H.K., "Microscopy of chemical-potential variations on an atomic scale", *Nature*, vol. 344, 1990, pp. 317-319.
[10] Lyeo H.K., Khajetoorians A.A., Shi L., Pipe K.P., Ram R.J., Shakouri A., Shih C.K., "Profiling the thermoelectric power of semiconductor junctions with nanometer resolution", *Science*, vol. 303, 2004, pp. 816-818.
[11] Sze S.M., *Semiconductor Devices, Physics and Technology*, John Wiley & Sons, 1985, Chap. 5.
[12] Salleh F., Asai K., Ishida A., Ikeda H., "Seebeck coefficient of ultrathin silicon-on-insulator layers", *Appl. Phys. Express*, vol. 2, 2009, pp. 071203-1-3.